

Strain-induced dimensionality crossover of precursor modulations in Ni₂MnGa

Zhihua Nie, Yandong Wang, Shunli Shang, Qiaoshi Zeng, Yang Ren, Dongmei Liu, Wenge Yang, Yi Wang, and Zi-Kui Liu

Citation: *Applied Physics Letters* **106**, 021910 (2015); doi: 10.1063/1.4906333

View online: <http://dx.doi.org/10.1063/1.4906333>

View Table of Contents: <http://scitation.aip.org/content/aip/journal/apl/106/2?ver=pdfcov>

Published by the **AIP Publishing**

Articles you may be interested in

[Coherent phonon dynamics at the martensitic phase transition of Ni₂MnGa](#)

Appl. Phys. Lett. **100**, 261911 (2012); 10.1063/1.4730946

[Large internal stress-assisted twin-boundary motion in Ni₂MnGa ferromagnetic shape memory alloy](#)

Appl. Phys. Lett. **99**, 141907 (2011); 10.1063/1.3645626

[Strain-induced dimensionality crossover and associated pseudoelasticity in the premartensitic phase of Ni₂MnGa](#)

Appl. Phys. Lett. **97**, 171905 (2010); 10.1063/1.3506508

[Large field induced strain in single crystalline Ni–Mn–Ga ferromagnetic shape memory alloy](#)

J. Appl. Phys. **87**, 5774 (2000); 10.1063/1.372518

[Magnetic-field-induced strain in Ni₂MnGa shape-memory alloy \(abstract\)](#)

J. Appl. Phys. **81**, 5416 (1997); 10.1063/1.364556

You don't still use this cell phone

or this computer

Why are you still using an AFM designed in the 80's?

It is time to upgrade your AFM

Minimum \$20,000 trade-in discount for purchases before August 31st

Asylum Research is today's technology leader in AFM

dropmyoldAFM@oxinst.com

OXFORD
INSTRUMENTS
The Business of Science®



Strain-induced dimensionality crossover of precursor modulations in Ni₂MnGa

Zhihua Nie,^{1,a)} Yandong Wang,^{2,a)} Shunli Shang,³ Qiaoshi Zeng,⁴ Yang Ren,⁵ Dongmei Liu,⁶ Wenge Yang,^{4,7} Yi Wang,³ and Zi-Kui Liu³

¹School of Materials Science and Engineering, Beijing Institute of Technology, Beijing 100081, China

²State Key Laboratory for Advanced Metals and Materials, University of Science and Technology Beijing, Beijing 100083, China

³Department of Materials Science and Engineering, The Pennsylvania State University, University Park, Pennsylvania 16802, USA

⁴High Pressure Synergetic Consortium (HPSynC), Geophysical Laboratory, Carnegie Institution of Washington, Argonne, Illinois 60439, USA

⁵X-Ray Science Division, Argonne National Laboratory, Argonne, Illinois 60439, USA

⁶State Key Laboratory for Fabrication and Processing of Nonferrous Metals, General Research Institute for Nonferrous Metals, Beijing 100088, China

⁷Center for High Pressure Science and Technology Advanced Research (HPSTAR), Pudong, Shanghai 201203, China

(Received 16 December 2014; accepted 8 January 2015; published online 16 January 2015)

Precursor modulations often occur in functional materials like magnetic shape memory alloys, ferroelectrics, and superconductors. In this letter, we have revealed the underlying mechanism of the precursor modulations in ferromagnetic shape memory alloys Ni₂MnGa by combining synchrotron-based x-ray diffraction experiments and first-principles phonon calculations. We discovered the precursor modulations along [011] direction can be eliminated with [001] uniaxial loading, while the precursor modulations or premartensite can be totally suppressed by hydrostatic pressure condition. The TA₂ phonon anomaly is sensitive to stress induced lattice strain, and the entire TA₂ branch is stabilized along the directions where precursor modulations are eliminated by external stress. Our discovery bridges precursor modulations and phonon anomalies, and sheds light on the microscopic mechanism of the two-step superelasticity in precursor martensite. © 2015 AIP Publishing LLC. [<http://dx.doi.org/10.1063/1.4906333>]

The fascinating precursor effect is a frequent phenomenon in first-order displacive crystalline structural transitions. It has been widely observed in the thermoelastic martensites like shape memory alloys,¹ high-T_C cuprates,² and ferroelectric ceramics,³ which are materials of different physical natures. Rod-like diffuse scattering, sharp satellite spots, and strain modulations (so-called tweed pattern) are often observed with x-ray diffraction and transmission electron microscopy when approaching the martensitic transition, which is accompanied by superelasticity, anomalous thermal expansion, elastic softening, specific heat, and so on.^{4–6} There exist alternative theoretical models on the physical origin of precursor modulations: (1) adaptive modulation constructed from nano-twinned martensite with tetragonal crystal structure,^{7,8} (2) micromodulation of cubic lattice related to the phonon anomaly,^{9,10} and (3) local strain field from statistical compositional fluctuations.^{11,12} Despite considerable experimental and theoretical research, the nature of precursor phenomenon is still in dispute.

Ni₂MnGa ferromagnetic shape memory alloys possess a thermoelastic martensitic transition coupled with a long-range magnetic ordering. They have received considerable research attentions due to their great physical properties, like magnetic shape memory,¹³ magnetocaloric,¹⁴ and

magnetostrictive.¹⁵ Precursor phenomenon (or premartensitic transition) has been observed in Ni₂MnGa alloys.^{16,17} Through stress-strain measurements, the peculiar interesting two-step superelastic behavior with a narrow hysteresis has been reported in the premartensite of Ni₂MnGa alloys.¹⁸ A uniaxial stress induced phase, named as X-phase, is suggested in the deformation map.¹⁹ This peculiar superelasticity in premartensite has been related to reversible redistribution of the precursor modulations from three-dimension to two-dimension under the applied uniaxial stress.²⁰ However, the physical mechanism on the change in modulation dimensionality is still unknown. It can hardly be explained simply by the reorientation of nanotwinned tetragonal martensitic variants, as the detwinning process should be normally irreversible and produces plastic deformation in alloys.²¹ The premartensitic transition indeed occurs in Ni₂MnGa intermetallic compounds with near-stoichiometric composition. After high temperature heat treatment for a long time, the composition inhomogeneity can be completely neglected.²²

In this letter, by combining *in-situ* synchrotron x-ray diffraction and first-principles phonon calculations, we studied the premartensitic transition in Ni₂MnGa alloys induced by both temperature and external stress/pressure. In contrast with thermo induced premartensite, the precursor modulations can be eliminated along certain crystal directions under uniaxial stress, for example, [011]_P and its equivalent

^{a)}Authors to whom correspondence should be addressed. Electronic addresses: zhihua_nie@yahoo.com and ydwang@neu.edu.cn.

directions when $[001]_P$ is the loading direction (LD) (P denotes the parent phase). When applying hydrostatic pressure, the precursor modulations or the premartensite are totally suppressed. First-principles calculations indicate that the TA_2 phonon anomaly is sensitive to stress induced lattice strain. The applied stress is able to stabilize the entire TA_2 branch along the same directions where precursor modulations are eliminated. Our results provide direct evidences confirming that the precursor modulations in Ni_2MnGa alloys are directly related to phonon anomalies.

A near-stoichiometric Ni_2MnGa single crystal was prepared through a floating-zone method and was described previously.²⁰ The premartensitic and martensitic transition temperatures of this system were detected to be ~ 230 K and ~ 175 K by using a superconducting quantum interference device (SQUID). High energy synchrotron *in-situ* x-ray diffraction experiments were performed at Advanced Photon Source, Argonne National Laboratory, to monitor the structural evolutions of the Ni_2MnGa crystal as a function of temperature, uniaxial stress, and hydrostatic pressure. First-principles phonon calculations were performed by using the supercell method²³ with the force constants calculated by the Vienna Ab-initio Simulation Package (VASP)²⁴ and the phonon properties predicted by Yphon code.²⁵ Detailed experimental procedures and calculation methods can be found elsewhere.²⁶

Figures 1(a)–1(f) show the series of two-dimensional (2D) x-ray diffraction patterns from the Ni_2MnGa single crystal at the $(400)_P$ area as a function of temperature during cooling. Figure 1(a) gives the $(400)_P$ Bragg reflection spot of the parent phase at 300 K. Upon cooling to 217 K, six satellite spots start to appear around the $(400)_P$ reflection, as shown in Figure 1(b), suggesting the formation of the premartensite with precursor modulations. These satellite spots can be indexed using a propagation vector of $(1/3, 1/3, 0)$ with a three-layered modulated (3M) structure. Upon cooling to 188 K [see Figure 1(c)], the intensities of these satellite spots reach maximum. Splitting of original $(400)_P$ reflection and a set of martensite spots are developed on further cooling

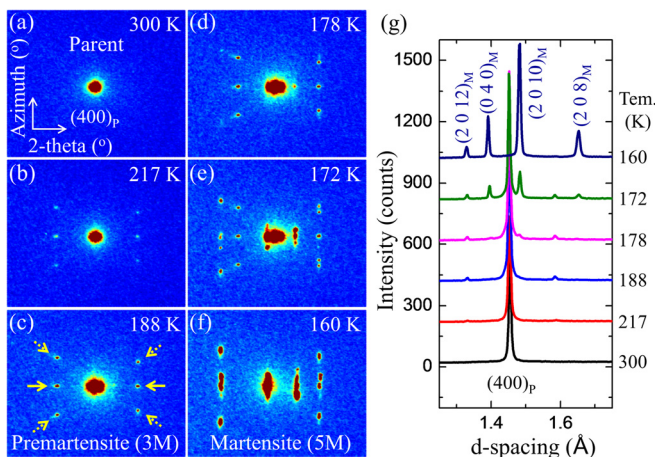


FIG. 1. Two-dimensional (a)–(f) and one-dimensional (g) diffraction patterns of a Ni_2MnGa single crystal collected at different temperatures. The solid and dotted arrows indicate out-plane and in-plane satellite diffraction spots, respectively. The *in-situ* x-ray diffraction experiment was performed at room temperature with photon energy of 115 keV.

as shown in Figures 1(d) and 1(e), which clearly reveal the thermo induced intermediate premartensite to martensite transition. Figure 1(f) shows the 2D diffraction pattern of the crystal at 160 K while the martensitic transition is completed. The integrated one-dimensional (1D) diffraction patterns are shown in Figure 1(g). The low-temperature martensite phase [Figure 1(g) at 160 K] can be assigned to the five-layered modulated (5M) martensite with $c/a = 0.94$, which is consistent with previous reports for near-stoichiometric Ni_2MnGa alloys.^{4,9,27}

The three dimensional (3D) distribution of the elastic diffuse scattering around $(400)_P$ Bragg reflection was recorded and constructed in reciprocal space at 300, 217, and 160 K as shown in Figure 2. A tungsten wafer was used to block the central $(400)_P$ Bragg reflection to allow to see the weak intensity around it. At 300 K, the diffuse directions are along $[440]_P$ and its equivalent directions. The diffuse scattering intensities increased with decreasing temperature down to 217 K and strong satellite points were generated at the scattering strips in a distance of $\sim 1/3$ magnitude of $\langle 110 \rangle_P$ lattice-vector from the main Bragg diffraction. Therefore, the six premartensitic satellite spots in Figure 1(c) can be classified into two groups, remarked by solid and dashed arrows. The solid arrow group represents four satellite spots on the $hk0$ plane and the dashed arrow group represents those on the $h0l$ plane. Similar diffraction patterns have been observed in Ni_2MnGa and $NiAl$ alloys by using transmission electronic microscopy.^{28,29} High resolution electron microscopy reveals that the rod-like diffuse scattering is due to the heterogeneous strain field, and the premartensitic satellite spots are attributed to micromodulation in six successive $\{110\}$ planes in the $\langle 1\bar{1}0 \rangle$ directions.^{28,29}

To understand the stress effect on the premartensitic and martensite transition, uniaxial compressive deformation was conducted on the Ni_2MnGa single crystal at room temperature with a strain-control mode along the $[001]_P$ direction

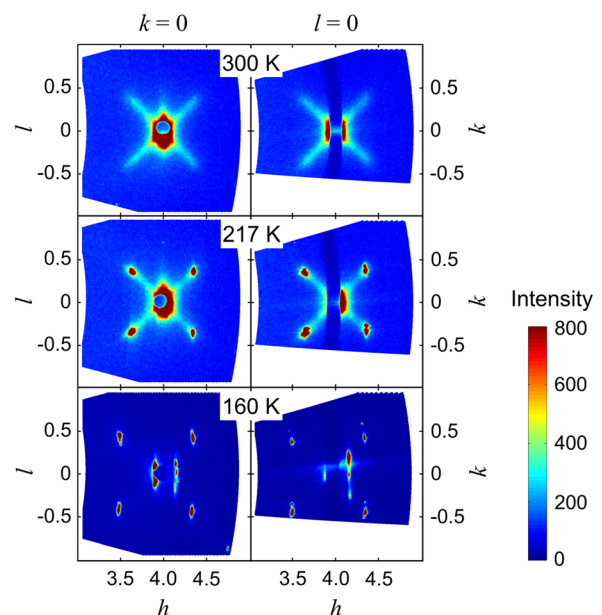


FIG. 2. Two-dimensional diffuse scattering patterns of parent phase, premartensite (3M) and martensite (5M), which were collected at 300 K, 217 K, and 160 K, respectively.

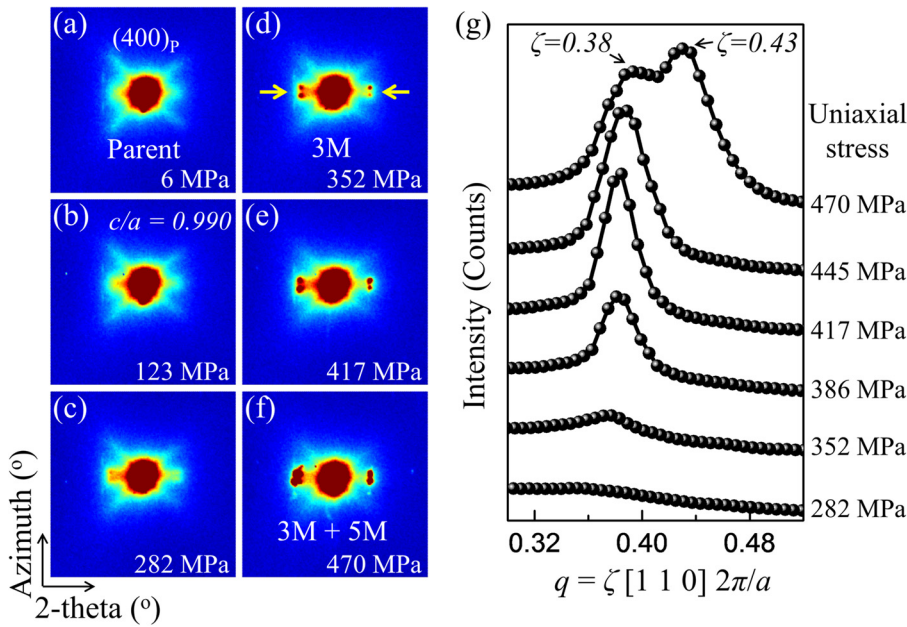


FIG. 3. Two-dimensional diffraction patterns of a Ni_2MnGa single crystal collected during loading at different uniaxial stresses (a)–(f) and reciprocal lattice-vector, q , for the premartensitic satellite spots as a function of stress during uniaxial compressive loading (g). The *in-situ* x-ray diffraction experiment was performed at room temperature with photon energy of 115 keV.

(with a deviation of $\sim 10^\circ$). Figures 3(a)–3(f) show a series of 2D scattering patterns for the $(400)_p$ area at each stress during loading. The uniaxial stress induced a tetragonal distortion of the parent cubic lattice with $a=b>c$, where c -axis is along the LD. The c/a ratios shown in Figure 3(b) are evaluated through the diffraction measurements from $(004)_p$ and $(400)_p$ reflections. With increasing stress to 352 MPa [see Figures 3(a)–3(d)], the premartensitic transition could be clearly observed from the generation of premartensitic satellite spots. It should be noted that the generated premartensitic satellite spots [indicated by solid arrows in Figure 3(d)] existed only on the peculiar reciprocal plane, i.e., $hk0$ plane, which is perpendicular to the LD. The premartensitic satellite spots on the $h0l$ plane, i.e., parallel to the LD, did not appear. The $(400)_p$ main spot and premartensitic satellite spots got split when the stress was increased to 470 MPa [see Figure 3(f)], which suggests a stress induced phase transition. The reciprocal lattice-vector (q) of the premartensitic satellite spots on $hk0$ plane was evaluated along $[110]_p$, which is shown in Figure 3(g) under different uniaxial stresses. The intensity of the premartensitic satellite peaks increases as increasing stress to 445 MPa. At 470 MPa a peak was produced with $\zeta=0.43$, which is in agreement with the reported q vector for the thermo induced 5M martensite phase in Ni_2MnGa alloys.^{4,9,27}

In-situ high energy x-ray diffraction experiments provide direct evidence that both thermo and uniaxial stress could induce phase transition in Ni_2MnGa alloys from parent to premartensite (3M) and then to a modulated martensite (5M). However, the uniaxial stress induced precursor modulations in premartensite are dimensionality crossover from 3D to 2D. In specific, the uniaxial stress induced structural modulations only appear on the lattice planes perpendicular to LD. In order to fully understand the experimental observations and reveal the physical origin of the modulation dimensionality crossover in Ni_2MnGa alloys, first-principles investigations of phonon dispersion have been performed in the tetragonally distorted Heusler structures with c/a from 0.94 to 1.2. Figures 4(a) and 4(b) show the predicted $[110]$

and $[011]$ phonon dispersions for Ni_2MnGa in the tetragonal structures with $c/a=0.99$, corresponding to the situation of uniaxial compressive deformation on the parent phase at 123 MPa [see Figure 3(b)] having c -axis along LD. It is clear that the anomalous TA_2 mode is substantially affected by the tetragonal distortion. Along $[110]$ direction, which is perpendicular to LD, the phonon anomaly (softening) is pronounced at q vector of $\zeta \approx 0.33$ [imaginary phonon frequency, see Figure 4(a)]. This q value is in agreement with the wave vector of precursor modulation observed experimentally. The imaginary phonon frequency indicates lattice instability. The structure can gain energy by moving the atoms along an eigenvector belonging to the imaginary phonons.^{10,30} However, along $[011]$ direction [see Figure 4(b)], the softening has completely disappeared and the entire TA_2 branch is

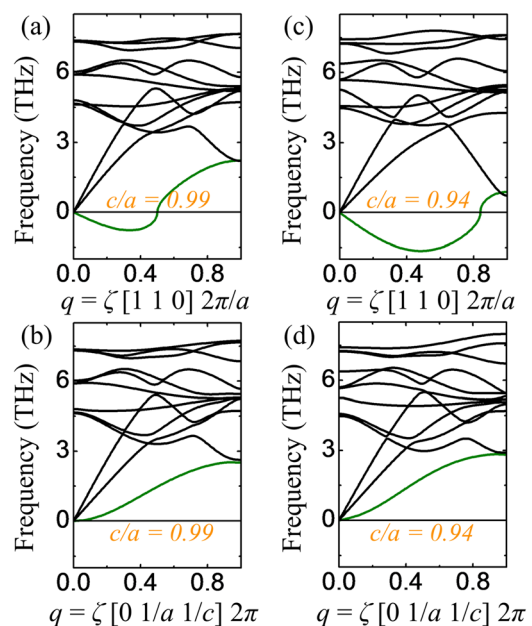


FIG. 4. First-principles $[110]$ and $[011]$ phonon dispersions for the Ni_2MnGa in the tetragonal structures with c/a ratios equal to 0.99 (a) and (b) and 0.94 (c) and (d).

stable. The above theoretical calculations on uniaxial stress induced redistribution of phonon populations reveal the physical origin of the observed modulation dimensionality crossover in premartensite. The observed 5M martensite phase has $c/a=0.94$ with q vector of $\zeta \approx 0.43$. The first-principles [110] and [011] phonon dispersions with $c/a=0.94$ are displayed in Figures 4(c) and 4(d). The phonon softening in TA_2 mode is much pronounced at q vector of $\zeta \approx 0.43$ along [110] direction and the anomaly has completely disappeared along [011] direction, which agrees with the reported quasi-1D-like modulation in 5M martensite.⁹

The uniaxial stress could eliminate the phonon softening along certain crystallographical directions, i.e., [011] and its equivalent directions like $[0\bar{1}1]$, $[101]$, and $[10\bar{1}]$, when [001] is along LD. Consequently, precursor modulations do not appear along those directions. The immediate question is what happens if a hydrostatic pressure is applied on this system. Will the hydrostatic pressure eliminate the phonon softening along all $\langle 110 \rangle$ directions and further suppress precursor modulations? In order to answer those questions, we have performed additional XRD experiments on the Ni_2MnGa alloy at a quasi-hydrostatic pressure environment using a symmetrical diamond anvil cell. The load sample is a highly textured Ni_2MnGa polycrystalline with $\langle 111 \rangle_p$ along incident x-ray beam. Figure 5(a) shows a series of diffraction patterns from the Ni_2MnGa powder under pressures from 0.2 GPa to 19 GPa. Previous observed diffraction peaks between 1.3 Å and 1.7 Å (premartensite and 5M martensite phases) did not show up in this pressure range, instead the Ni_2MnGa parent phase is gradually transformed to a non-modulated (NM) tetragonal martensite phase under quasi-hydrostatic pressure. The lattice parameters and unit cell volume as a function of pressure are shown in Figures 5(b) and 5(c), respectively. As seen in Figure 5(c), the unit cell volume decreases as increasing pressure, and a discontinuity in volume appears at ~ 10 GPa where the parent to NM martensite phase transition takes place. The c/a ratio for the NM martensite changes from 1.20 to 1.23 when the pressure is

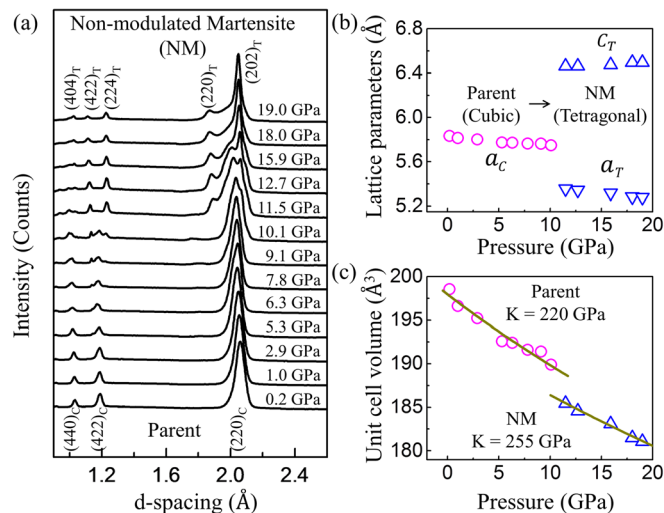


FIG. 5. One-dimensional diffraction patterns of a Ni_2MnGa polycrystalline at different quasi-hydrostatic pressures (a), lattice parameters (b), and unit cell volume (c) as a function of pressure. The *in-situ* x-ray diffraction experiment was performed at room temperature with photon energy of 30 keV.

increased to 19 GPa. Following the equation of state, the bulk moduli for the parent and NM martensite phase are calculated to be 220 GPa and 255 GPa, respectively. Our high-pressure experiment indicates that the hydrostatic pressure may suppress the phonon softening modes. We have conducted the first-principles [110] phonon dispersions study for Ni_2MnGa with $c/a=1.2$ (NM martensite). We find that the entire TA_2 soft modes are stable along [110] direction, which is in good agreement with previous first-principles results.¹⁰

Our experiments and calculations provide the microscopic view on the stress-induced crossover in dimension of modulations for the precursor martensite. The anisotropy in phonon softening modes under uniaxial stress field should be closely related to a kind of continuous transition from one unfavorable low-crystal-symmetry domain to another favorable one.^{31,32} As the total free energy altered by different phonon vibration modes is not so large, a low elastic modulus can be predicted via the domain-switch mechanism.²⁰ The transition in phonon softening modes caused by the uniaxial stress field is accomplished by a small atomic displacement, which is analogous to the stress-induced structural transition between the two low-crystal-symmetry domains; thus, a giant low- or non-hysteretic stress-field-induced response in the Ni_2MnGa precursor martensite may be maintained.

In summary, in this letter we report the mechanism of stress-induced modulation dimensionality crossover in Ni_2MnGa premartensite. Based on first-principles phonon dispersion calculations, we conclude that the modulation dimensionality crossover is due to redistribution of phonon populations in the TA_2 branch under external stress. Importantly, the uniaxial stress induced redistribution of phonon populations is reversible upon releasing the loading. Our discovery bridges precursor modulations and phonon anomalies, and sheds light on the microscopic mechanism of the two-step superelasticity in precursor martensite.

This work was supported by the National Basic Research Program of China (973 Program) under Contract No. 2012CB619405. S.L.S., Y.W., and Z.K.L. would like to thank the support from U.S. NSF with Grant Nos. DMR-1006557 and DMR-1310289. HPSynC was supported by the EFree, an Energy Frontier Research Center funded by DOE-BES under Grant DE-SC0001057. The x-ray studies were conducted on beam lines 11ID-C and HPCAT 16BM-D at the Advanced Photon Source. HPCAT operations are supported by DOE-NNSA under Award DE-NA0001974 and DOE-BES under Award DE-FG02-99ER45775, with partial instrumentation funding by NSF. Use of the Advanced Photon Source was supported by the U.S. DOE, Office of Science, Office of Basic Energy Sciences, under Contract No. DE-AC02-06CH11357.

¹K. Otsuka and X. Ren, *Prog. Mater. Sci.* **50**, 511 (2005).

²S. Chakravarty, R. B. Laughlin, D. K. Morr, and C. Nayak, *Phys. Rev. B* **63**, 094503 (2001).

³W. Eerenstein, N. D. Mathur, and J. F. Scott, *Nature (London, U.K.)* **442**, 759 (2006).

⁴A. Zheludev, S. M. Shapiro, P. Wochner, and L. Tanner, *Phys. Rev. B* **54**, 15045 (1996).

- ⁵C. M. Hwang, M. Meichle, M. B. Salamon, and C. M. Wayman, *Philos. Mag. A* **47**, 9 (1983).
- ⁶D. Viehland, *J. Appl. Phys.* **88**, 4794 (2000).
- ⁷A. G. Khachatryan, S. M. Shapiro, and S. Semenovskaya, *Phys. Rev. B* **43**, 10832 (1991).
- ⁸S. Kaufmann, U. K. Röbber, O. Heczko, M. Wuttig, J. Buschbeck, L. Schultz, and S. Fähler, *Phys. Rev. Lett.* **104**, 145702 (2010).
- ⁹C. P. Opeil, B. Mihaila, R. K. Schulze, L. Mañosa, A. Planes, W. L. Hults, R. A. Fisher, P. S. Riseborough, P. B. Littlewood, J. L. Smith, and J. C. Lashley, *Phys. Rev. Lett.* **100**, 165703 (2008).
- ¹⁰M. A. Uijtewaal, T. Hickel, J. Neugebauer, M. E. Gruner, and P. Entel, *Phys. Rev. Lett.* **102**, 035702 (2009).
- ¹¹S. Kartha, J. A. Krumhansl, J. P. Sethna, and L. K. Wickham, *Phys. Rev. B* **52**, 803 (1995).
- ¹²A. Saxena, T. Castán, A. Planes, M. Porta, Y. Kishi, T. A. Lograsso, D. Viehland, M. Wuttig, and M. De Graef, *Phys. Rev. Lett.* **92**, 197203 (2004).
- ¹³K. Ullakko, J. K. Huang, C. Kantner, R. C. O'Handley, and V. V. Kokorin, *Appl. Phys. Lett.* **69**, 1966 (1996).
- ¹⁴J. Marcos, L. Mañosa, A. Planes, F. Casanova, X. Batlle, and A. Labarta, *Phys. Rev. B* **68**, 094401 (2003).
- ¹⁵C. Biswas, R. Rawat, and S. R. Barman, *Appl. Phys. Lett.* **86**, 202508 (2005).
- ¹⁶A. Planes, E. Obrado, A. Gonzalez-Comas, and L. Manosa, *Phys. Rev. Lett.* **79**, 3926 (1997).
- ¹⁷V. A. Chernenko, J. Pons, C. Segui, and E. Cesari, *Acta Mater.* **50**, 53 (2002).
- ¹⁸I. Karaman, H. E. Karaca, B. Basaran, D. C. Lagoudas, Y. I. Chumlyakov, and H. J. Maier, *Scr. Mater.* **55**, 403 (2006).
- ¹⁹J. H. Kim, T. Fukuda, and T. Kakeshita, *Scr. Mater.* **54**, 585 (2006).
- ²⁰Z. H. Nie, Y. Ren, Y. D. Wang, D. M. Liu, D. E. Brown, G. Wang, and L. Zuo, *Appl. Phys. Lett.* **97**, 171905 (2010).
- ²¹L. Lu, Y. F. Shen, X. H. Chen, L. H. Qian, and K. Lu, *Science* **304**, 422 (2004).
- ²²P. J. Brown, J. Crangle, T. Kanomata, M. Matsumoto, K.-U. Neumann, B. Ouladdiaf, and K. R. A. Ziebeck, *J. Phys.: Condens. Matter* **14**, 10159 (2002).
- ²³A. van de Walle and G. Ceder, *Rev. Mod. Phys.* **74**, 11 (2002).
- ²⁴G. Kresse and J. Furthmüller, *Phys. Rev. B* **54**, 11169 (1996).
- ²⁵Y. Wang, J. J. Wang, W. Y. Wang, Z. G. Mei, S. L. Shang, L. Q. Chen, and Z. K. Liu, *J. Phys.: Condens. Matter* **22**, 202201 (2010).
- ²⁶See supplementary material at <http://dx.doi.org/10.1063/1.4906333> for detailed experimental procedures and calculation methods.
- ²⁷U. Stuhr, P. Vorderwisch, V. V. Kokorin, and P.-A. Lindgard, *Phys. Rev. B* **56**, 14360 (1997).
- ²⁸D. Schryvers and L. E. Tanner, *Ultramicroscopy* **32**, 241 (1990).
- ²⁹K. Tsuchiya, Y. Todaka, and M. Umemoto, *Mater. Sci. Technol.* **24**, 920 (2008).
- ³⁰A. T. Zayak, P. Entel, J. Enkovaara, A. Ayuela, and R. M. Nieminen, *Phys. Rev. B* **68**, 132402 (2003).
- ³¹W.-F. Rao, M. Wuttig, and A. G. Khachatryan, *Phys. Rev. Lett.* **106**, 105703 (2011).
- ³²Y. M. Jin, Y. U. Wang, Y. Ren, F. D. Ma, J. E. Zhou, T.-L. Cheng, B. L. Wang, L. D. Geng, and I. A. Kuyanov, "Broken dynamic symmetry and phase transition precursor," arXiv:1302.5479.